Conductance and Ion Selectivity of a Mesoscopic Protein Nanopore Probed with Cysteine Scanning Mutagenesis

Petr G. Merzlyak,* Maria-Fatima P. Capistrano,† Angela Valeva,‡ John J. Kasianowicz,§ and Oleg V. Krasilnikov*
*Laboratory of Membrane Biophysics, Department of Biophysics and Radiobiology, Universidade Federal de Pernambuco, Recife, Pernambuco, Brazil; †Department of Biophysics and Pharmacology, Federal University of Rio Grande de Norte, Natal, Rio Grande de Norte, Brazil; ‡Institute of Medical Microbiology and Hygiene, University of Mainz, Germany; and §National Institute of Standards and Technology, Electronics and Electrical Engineering Laboratory, Semiconductor Electronics Division, Gaithersburg, Maryland 20899-8120

ABSTRACT Nanometer-scale proteinaceous pores are the basis of ion and macromolecular transport in cells and organelles. Recent studies suggest that ion channels and synthetic nanopores may prove useful in biotechnological applications. To better understand the structure-function relationship of nanopores, we are studying the ion-conducting properties of channels formed by wild-type and genetically engineered versions of *Staphylococcus aureus* α-hemolysin (αHL) reconstituted into planar lipid bilayer membranes. Specifically, we measured the ion selectivities and current-voltage relationships of channels formed with 24 different αHL point cysteine mutants before and after derivatizing the cysteines with positively and negatively charged sulfhydryl-specific reagents. Novel negative charges convert the selectivity of the channel from weakly anionic to strongly cationic, and new positive charges increase the anionic selectivity. However, the extent of these changes depends on the channel radius at the position of the novel charge (predominately affects ion selectivity) or on the location of these charges along the longitudinal axis of the channel (mainly alters the conductance-voltage curve). The results suggest that the net charge of the pore wall is responsible for cation-anion selectivity of the αHL channel and that the charge at the pore entrances is the main factor that determines the shape of the conductance-voltage curves.

INTRODUCTION

By virtue of their action in nerve, muscle, and other tissues (1), protein ion channels are of key importance in biology. Recent work suggests that channels (2–11) and solid-state analogs (12–15) might prove useful in technological applications, which include rapid DNA sequencing and the simultaneous detection of multiple analytes. However, more insight into how channels catalyze ion and macromolecule transport is needed to aid the rational design of nanopore-based sensors.

Ion channels are an ideal model system for the study of nanopores because they self-assemble, and their structures can be altered using molecular biological techniques. For example, site-directed mutagenesis can be used to change the number and location of fixed charges inside the channel and/or near the pore entrances. The effects of such changes to the channel structure are generally reflected in the ion selectivity and the shape of the *I-V* relationship (16–20). To learn more about how charged amino acid side chains control the properties of ion channels, we studied the conducting properties of the channel formed by the bacterial exotoxin *Staphylococcus aureus* α-hemolysin (αHL) (21) and its genetically engineered mutants.

The αHL channel forms spontaneously from seven identical monomers (22–24), each with a molecular mass of 33.1 kDa. The crystal structure of the αHL channel was determined nearly a decade ago (23). The channel, illustrated in (Fig. 1 *A*) is ~10 nm long. It is comprised of a large cap domain and a much less massive stem region. The stem, which spans the lipid bilayer, is an almost cylindrical 14-stranded β-barrel with an average diameter of ~2.6 nm between α-carbons on opposite sides of the pore (23,25,26). Both ends of the stem are decorated with rings of acidic and basic residues separated by a 4-nm stretch of neutral amino acids. The cap domain is extramembranous (27,28) and contains a vestibule with a maximum diameter of ~4.6 nm (23,29). The cap and stem are separated by a constriction with a diameter ~1.2 nm (23,30,31). Both openings of the channel are relatively large (diameter ~2.6 nm) (30).

By virtue of its relatively large internal lumen and the location of fixed charges inside the pore, the αHL channel is only weakly anion-selective and exhibits a mildly nonlinear and asymmetric current-voltage relationship (32–35). In contrast, narrow channels are likely to be dominated by electrostatic interactions between pore-permeant ions and the channel wall that results in a high degree of ion selectivity (36). Because the αHL channel has both wide and narrow regions inside its pore, it is an excellent candidate for ion selectivity studies.

The single αHL nanopore has also been used to study the transport of neutral (25,37–39) and charged polymers (5,11,40,41). Curiously, the charge state of ionizable amino

Submitted May 12, 2005, and accepted for publication July 26, 2005.

Address reprint requests to Dr. Oleg V. Krasilnikov, Universidade Federal de Pernambuco, Centro de Ciências Biológicas, Depto. de Biofísica e Radiobiologia, Av. prof. Moraes Rego, S/N, Cidade Universitária, Recife, Pernambuco, Brasil, CEP 50670-901. Tel.: 55-81-2126-8535; Fax: 55-81-2126-8560; E-mail: kras@ufpe.br.

0006-3495/05/11/3059/12 $2.00

doi: 10.1529/biophysj.105.066472

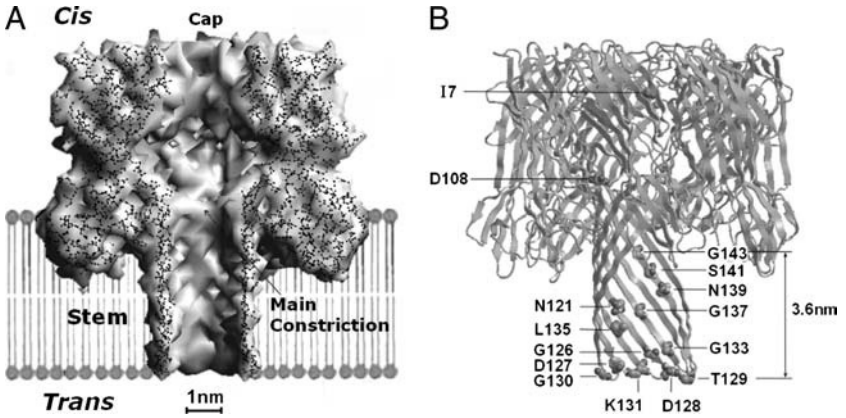

FIGURE 1 Molecular models of αHL. (*A*) Schematic illustration of sagittal section through the heptameric αHL pore inserted in lipid bilayer. The cartoon shows the relative sizes of the pore, the positions of the main constriction, cap, and stem regions of the channel in the lipid bilayer. (*B*) Ribbon representation of the αHL pore. The positions some of amino acids, which are the loci for the substitutions described herein are shown in the space-filled representation. The longitudinal section and the ribbon representation of αHL channel (Protein Data Bank code 7AHL.pdb) were visualized with CS Chem3D Pro (CambridgeSoft). The final representations were produced with Adobe Photoshop.

acid side chains on the channel affects the dynamic partitioning of neutral polymers into the pore (42).

Our objective here was to determine the significance of the type and location of fixed charges on the selectivity, conductance (*G*), and *G-V* dependence of the αHL channel. The pioneering work by Akabas and colleagues demonstrated that cysteine scanning mutagenesis could be used to map the topology of an ion channel (43). Because the primary sequence of wild-type αHL has no cysteines, we produced many point cysteine mutants and determined their effects on the conducting properties of the αHL channel. The positions for some of these substitutions are shown in Fig. 1 *B*. We subsequently chemically modified these novel cysteine side chains with water-soluble sulfhydryl-specific reagents. The results suggest that the net charge of the channel wall is responsible for cation-anion selectivity of the αHL channel, whereas the balance of charges between the openings is the major determinant for the shape of the conductance-voltage curves.

MATERIALS AND METHODS

1,2-Diphytanoyl-*sn*-glycero-3-phosphatidylcholine (DiPhyPC) was purchased from Avanti Polar Lipids (Alabaster, AL). Cholesterol, dithiothreitol (DTT), and 5,5′-dithio-bis-(2-nitrobenzoic acid) (DTNB) were purchased from Sigma Chemical (St. Louis, MO). 2-Sulfonatoethyl methanethiosulfonate (MTSES), 2-(trimethylammonium) ethyl methanethiosulfonate (MTSET), and 2-aminoethyl methanethiosulfonate (MTSEA), derivatives of methanethiosulfonate, were purchased from Toronto Research Chemicals (North York, Ontario, Canada). The other chemicals used in this study were analytical grade.

Electrophysiological measurements

Planar lipid bilayer membranes were formed as described elsewhere (39,44). Briefly, the two compartments of the Teflon cell were separated by a 25-μm-thick Teflon partition with an ~300-μm-diameter orifice that was pretreated with a 1% solution of hexadecane in *n*-pentane. DiPhyPC was dissolved at 5 mg/ml in pentane or hexane and spread at the air-water interface of the aqueous buffered solutions on both sides of the partition. Membranes were formed on the orifice by sequentially raising the level of the aqueous electrolyte solutions.

Channel-forming proteins were added to one side of the chamber (herein defined as *cis*). A negative applied electrostatic potential drives anions from the *cis* to the *trans* chamber. The membrane potential was maintained using Ag/AgCl electrodes in 3000 mM KCl, 3% agarose bridges. Milli-Q plus treated water (Millipore, Bedford, MA) with resistivity of 18 MΩ cm was used to prepare all buffer solutions. Unless stated otherwise, the standard solution contained 100 mM KCl, 1 mM DTT, and 30 mM Tris adjusted to pH 7.5 with HCl. The channel conductance, *G*, was measured in the presence of symmetric electrolyte solutions. To determine the *G-V* curve for single channels, voltage pulses that lasted for several seconds were applied.

The ion selectivities of the channels were estimated in the presence of a threefold electrolyte concentration gradient (e.g., with 100 mM KCl present on the *trans* side and 300 mM KCl on the *cis* side, both buffered to pH 7.5 with 30 mM Tris HCl), as described elsewhere (45). The transmembrane potential that is required to null the ionic current is defined as the reversal potential, V_{rev}. All potentials were corrected for electrode asymmetry (usually <0.3 mV) and for liquid junction potentials (calculated using the Henderson equation (46). A positive value for V_{rev}, with respect to the side containing the greater electrolyte concentration, indicates an anion-selective channel. To estimate the relative permeability ratios (P_K/P_{Cl}), the Goldman-Hodgkin-Katz equation was employed. The P_{TRIS}/P_K was assumed to be equal to the ratio of their mobilities, $u_{TRIS}/u_K \sim 0.4$, (47).

The experiments were performed at room temperature (25 ± 2°C) under voltage-clamp conditions. The current was converted to voltage, digitized with a sampling frequency of 0.5 kHz, stored on a computer and analyzed off-line with the Whole Cell Electrophysiology Program (WCP V1.7b, J. Dempster, University of Strathclyde, Glasgow, UK).

Sulfhydryl reagents

The sulfhydryl reagents used in this study are small water-soluble sulfhydryl-specific reagents that have fixed positive or negative charges. They bind to cysteine side chains exposed to the aqueous phase. The reagents were usually applied to both compartments of the planar bilayer chamber at concentrations 0.5 mM, 2 mM, 1.0 mM, and 1.0 mM greater than the concentration of DTT in the solution for DTNB, MTSES, MTSET, and MTSEA, respectively. An increase in the reagent concentration over the values noted above caused no additional change in the values of the conducting properties of the channels reported below. The reaction of these reagents with a reduced cysteine side chain converts the −SH group to −SS-R, where R is the charged moiety, $-C_6H_3NO_2COO^-$ (DTNB), $-CH_2CH_2SO_3^-$ (MTSES), $-CH_2CH_2N(CH_3)_3^+$ (MTSET), or $-CH_2CH_2NH_3^+$ (MTSEA). The introduction of an additional charged group should affect the single-channel conductance if the chemically modified novel cysteine side chain either lines the channel lumen or is located adjacent to either channel entrance. A change in the channel conducting properties after

reagent application served as a criterion for judging the accessibility of the point cysteine mutant side chain to the sulfhydryl reagent (43).

αHL proteins

Wild type αHL and single cysteine-substitution αHL mutants were prepared as previously described (48). The following mutant proteins were constructed and isolated: I7C, D108C, Y118C, F120C, N121C, G122C, V124C, G126C, D127C, D128C, T129C, G130C, K131C, I132C, G133C, G134C, L135C, I136C, G137C, A138C, N139C, V140C, S141C, and G143C. The proteins were stored at −70°C in the presence (mutants) or absence (wild-type αHL) of 5 mM DTT. Before the electrophysiological experiments, the mutant versions of αHL were reduced by incubation with 30 mM DTT for 20 min. Stock solutions of the reduced proteins were then stored at 4°C for a maximum of 5 days, and diluted 10- to 50-fold before the experiments.

The positions of each amino acid side chain along the channel axis, with respect to the *trans* entrance, were estimated from the αHL channel crystallographic structure (7AHL.pdb) using Swiss-Pdb Viewer version 3.7 (49) and CS Chem3D Pro (CambridgeSoft, Cambridge, MA).

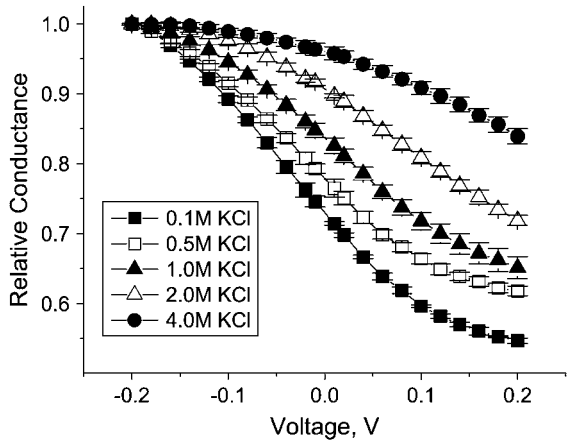

FIGURE 2 Voltage dependence of wild-type αHL channel conductance in the presence of different potassium chloride concentrations. The relative single-channel conductances, which are normalized at −200 mV transmembrane voltage, decrease as the applied potential is increased. In addition, an increase in the electrolyte concentration decreases the effect of voltage on the conductance. The electrolyte solutions are buffered with 5 mM Tris and adjusted to pH 7.5 with citric acid. Each point presents the mean value ± SD of at least seven separate experiments.

RESULTS AND DISCUSSION

Cysteine substitution and *G-V* dependencies of channels

Analytical studies (19,50,51) demonstrated that fixed charges on membrane surfaces (in the absence of channels) or inside channels could cause rectification of ionic current. Subsequent experiments on a K^+ channel (52) and the αHL channel (28,32,34,53) showed that the charge on the membrane surface could alter ion selectivity and the *G-V* relationship. Therefore, to exclude the effects of fixed charges on the membrane, we used zwitterionic phosphatidylcholine bilayers. The *trans* channel opening adjacent to one of the membrane surfaces (8,28) was used as a zero-position reference point.

The conductance, *G-V* lineshape, ion selectivity, and other αHL channel properties are sensitive to the pH and bathing solution electrolyte concentration (2,4,28,32,34,35,53–55). Fig. 2 demonstrates that increasing the 1:1 electrolyte concentration decreases the asymmetry (with respect to the sign of the applied potential) of the *G-V* curves for wild-type αHL channels. Interestingly, current rectification was observed even at 4000 mM KCl. These results suggest that the charges lining the pore walls mainly control the ability of mobile ions to be transported through the αHL channel (19). It follows that changes in the sign, magnitude, and/or position of charges lining the channel lumen result in changes to the local electrostatic environment and the channel conducting properties. To better reveal the role of these charges, in the majority of experiments, we used aqueous solutions with a relatively low ionic strength (i.e., 100 mM KCl) because the effective Debye length is large (~1 nm). The experiments are more difficult to carry out in solutions with even lower ionic strengths because the αHL channel tends to gate quickly (J. J.Kasianowicz, unpublished observation).

All of the αHL mutants reported here were divided into three groups. The first group included the mutants (I7C and D108C) with substitutions in the cap domain. Mutants in two other groups contained a novel cysteine at even-numbered positions or odd positions of the β-barrel stem region, respectively. In all cases, the addition of wild-type αHL or any of the mutants at concentrations of ~1–10 ng/ml to the *cis* aqueous compartment led to a stepwise increase in the ionic current (Fig. 3). Each step corresponds to the formation of a single channel.

αHL reconstitutes into the membrane in the same orientation each time, most likely because the large cap domain cannot traverse the membrane. The well-defined asymmetry in the αHL channel *G-V* curve (25,28,32,33) serves as a test of this *ansatz*. The αHL channel conductance, as determined from the step increases in current, varies slightly from channel to channel (see, e.g., Krasilnikov and colleagues (25,30, 32,41)). Therefore, we recorded the formation of several hundred individual (i.e., distinct) ion channel formation events. The step conductances were analyzed and used to build cumulative probability density amplitudes. Examples of an ionic current recording and the step current probability density amplitudes are shown in Fig. 3. The histograms usually have a well-defined peak that we fitted with a Gaussian curve. The value of the most probable channel conductance obtained for each mutant αHL is defined herein as a standard. Only the channels with a conductance close to this nominal value were used to study *G-V* dependencies in the single-channel experiments (i.e., we ignored the much less probable lower conductance states). When membranes containing many channels were used, the data were normalized to the

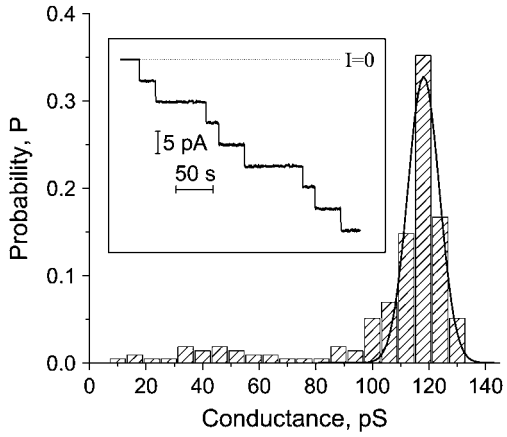

FIGURE 3 Conductance histogram of single channels formed by the genetically engineered protein αHL G134C. The inset illustrates a typical current recording of single channels spontaneously formed by G134C αHL monomer added to the *cis* compartment (final concentration ~5 ng/ml). Current records were not analyzed if any of the open channels closed temporarily (i.e., gated). The histogram is comprised of the conductance values of 210 channel formation events (5–15 channels per membrane) and the bin width is 6 pS. The solid line indicates the best fit of a single normal distribution to the most probable conductance values near 120 pS. The applied potential was −40 mV. All other conditions for the experiment are described in the Methods section.

number of channels present in the membrane. As was noted above, the αHL channel can gate from the fully open state to closed states (2,54,56–58). If a channel gating event occurred during the course of an experiment, we did not analyze subsequent step increases in current. Thus, we only present data that correspond to fully open channels.

Because Ohm's law is a reasonable first approximation for the ionic conductance of large channels, we expected the channel properties to depend on the type of αHL mutant. For example, a novel cysteine side chain could alter the channel conductance simply because its volume is different from the side chain it replaced. In addition, changes in the fixed charge distribution inside or near the pore would change the transmembrane electrostatic potential profile and, hence, the barriers and wells for pore-permeant mobile ions. Examples of *G-V* curves for the point cysteine mutants and wild-type αHL are presented in Fig. 4. Of the 24 mutants examined, only six mutations that are close to the *trans* channel entrance (i.e., amino acid side chains at positions 126, 128, 129, 130, 131, and 133 (Fig. 1 *A*)) have considerable influence on the channel conductance. Except at position 130 (see the experimental study of Krasilnikov et al. (53)) and positions 128 and 131 (see the theoretical study of Noskov et al. (19)), none of the other three mutations were reported to have a major effect on αHL channel properties without subsequent chemical modification. In addition, only the channel formed by D128C demonstrates an inversion in the conductance-voltage dependence. The latter result is consistent with the assumption (19) that D128, although presumably in a hydrophobic zone (see below), is in a charged form and contributes to the channel conductance rectification.

The *G-V* curves of the channels formed by other mutants were only slightly different from the control data for the wild-type αHL channel. Thus, novel cysteines at those positions did not significantly affect channel structure. To better visualize the effects of the amino acid substitutions, the asymmetry of the *G-V* curves at $\pm$100 mV is shown in Fig. 5.

The change in asymmetry (or rectification ratio, $G_{-100\ \mathrm{mV}}/G_{+100\ \mathrm{mV}}$) of the ion channel conductance is greater when the cysteine substitution is made closer to the *trans* pore entrance. This is true for the substitutions at both odd- and even-numbered positions in the β-barrel. The results for odd-numbered positions are sensible because the crystal structure suggests that the side chains of these amino acid residues face the pore lumen (23). The effectiveness of some cysteine substitutions at even-numbered positions is also plausible because they are close to the *trans* pore entrance and apparently not buried in the membrane.

In general, the point cysteine substitutions, except for D127C and D128C, increase the asymmetry of the G/V curves. An increase in the rectification ratio was observed for channels formed by mutants in which a positively charged (K131) or neutral residue (especially if it is close to the *trans* opening) was substituted with Cys having a weak negative charge. These results suggest that the electric charge magnitude and location affect the value of the ionic current rectification. The pKa of the cysteine sulfhydryl group is generally alkaline (59). Thus, at the pH value in the experiments reported here, the substitution of any neutral amino acid residue with cysteine would introduce a negative charge at the position. This novel charge should be less than that of the carboxyl group of Asp, because the pKa of Asp in the bulk is ~4 (i.e., several pH units lower than the pH of the solutions used in this study). Indeed, the *G-V* curve of the channel formed by D128C is significantly changed. Thus, we suggest that a negative charge close to the *trans* pore entrance increases the asymmetry in the G-V curve, whereas one close to the *cis* opening decreases it. A cysteine substitution at position 7 should therefore decrease the asymmetry of the *G-V* curve. However, this was not observed for channels formed by I7C; the weak negative charge of Cys was not strong enough to evoke a change because the diameter of the αHL channel at this location is considerably larger than that in the stem region. However, a distinct change was observed when a greater negative charge was introduced at this position by targeted chemical modification (24). The results suggest that the asymmetry (and the *G-V* curve) is mainly determined by the asymmetric distribution of charges in the two halves of the channel. Negative charge predominates in the *trans* opening, and positive charge predominates in the *cis* entrance. These findings are consistent with a recent theoretical study (19).

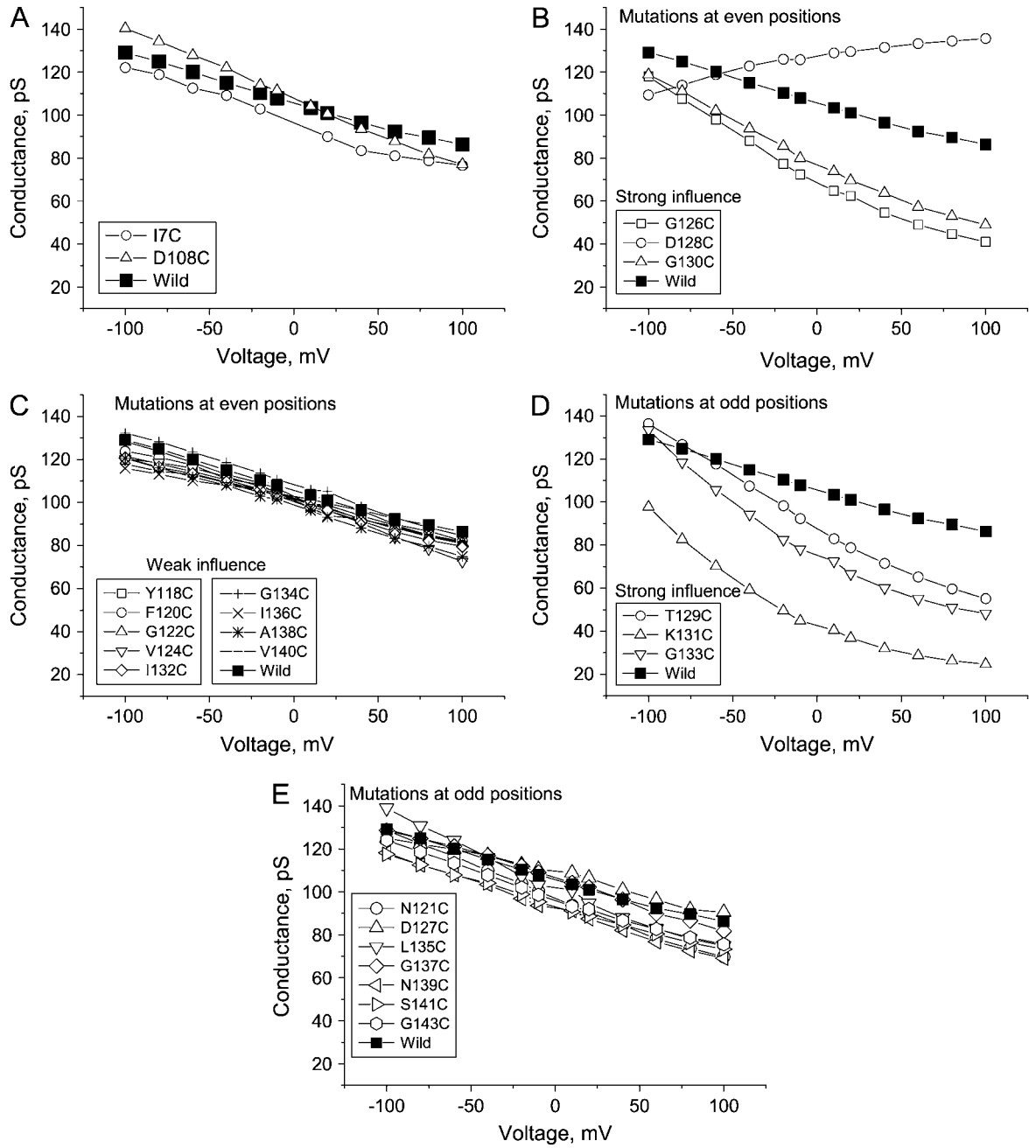

FIGURE 4 Steady-state conductance-voltage relationships of single channels formed by wild-type and novel point cysteine mutant versions of αHL. Each *G-V* data set represents the averages of 3–5 independent experiments. The standard deviations, which did not exceed 10% of the conductance values, are omitted for clarity.

Cysteine substitution and cation-anion selectivity of the channel

The results of cation-anion selectivity measurements for the channels formed by wild-type αHL and the mutant versions are summarized in Fig. 6. Cysteine substitution changed the channel selectivity, and the degree of the change depended on the location of the novel Cys. Point cysteine substitutions at odd-numbered positions caused a larger change in selectivity. However, mutations at several even-numbered positions also elicited changes in ion selectivity. These effects were greatest when the substitution was made close to the *trans* opening. Cysteine substitutions for negatively charged carboxyl groups of Asp-127 and Asp-128 increased the anion selectivity of the channel. All other substitutions led to a decrease in the anion selectivity or even reversed it (i.e., K131C, G133C, and G126C). The strong cation selectivity

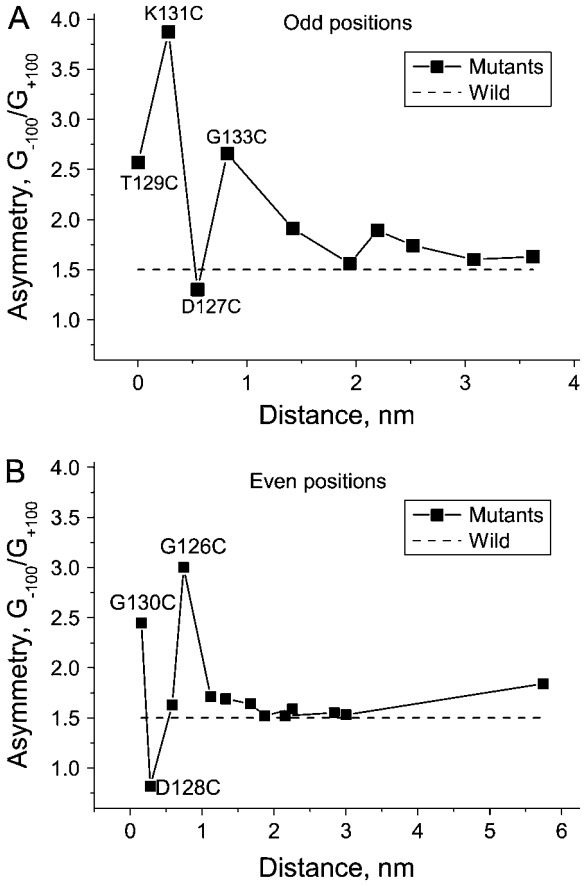

FIGURE 5 Effect of single cysteine substitutions on the αHL channel rectification. The dashed line represents the ratio of the conductance value at -100 mV to that at $+100$ mV (G_{-100}/G_{+100}) for the wild-type αHL channel. The abscissa denotes the distance between each novel cysteine side chain and *trans* channel opening. The sequences of mutants from left to right are (*A*) T129C, K131C, D127C, G133C, L135C, G137C, N121C, N139C, S141C, and G143C, and (*B*) G130C, D128C, I132C, G126C, G134C, V124C, I136C, G122C, A138C, F120C, V140C, and Y118C. The conductance rectification ratio of the channels formed by D108C and I7C (in the αHL channel cap region at 5.74 nm and 8.50 nm from the *trans* opening) are 1.81 ± 0.07 and 1.55 ± 0.06, respectively. Each point represents the mean value of G_{-100}/G_{+100} obtained in 3–5 separate experiments.

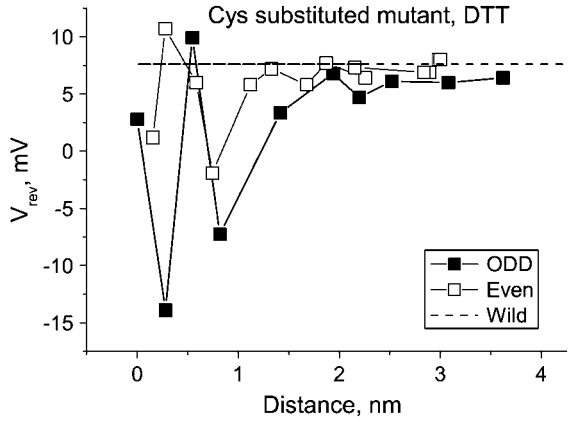

FIGURE 6 Effect of single cysteine substitutions on the reversal potential of αHL channels. The reversal potential was measured in the presence of a threefold KCl concentration gradient (300 mM *cis*, 100 mM *trans*) in the presence of 1 mM DTT and 30 mM Tris. The dashed line represents the value of the reversal potential for channels formed by wild-type αHL. The sequences of mutants from left to right are: odd, T129C, K131C, D127C, G133C, L135C, G137C, N121C, N139C, S141C, and G143C; and even, G130C, D128C, I132C, G126C, G134C, V124C, I136C, G122C, A138C, F120C, V140C, and Y118C. The reversal potentials of channels formed by D108C and I7C are 6.9 ± 0.9 and 6.4 ± 0.3, respectively. Each point represents the mean value of V_{rev} obtained in 5–7 separate experiments.

of the channel formed by K131C, the mutant with the most prominent change, is easy to explain. It results from the substitution of the positive charge of the Lys side chain with the weak negative charge of Cys. The effects due to G133C and G126C were moderate. Nevertheless, the introduction of even a weak negative charge at these positions impacts the channel ion selectivity. We cannot completely rule out the possibility that these substitutions also result in a local reorganization in stem structure. Cysteine substitutions in the cap region (D108C and I7C) made anion selectivity of the channel weaker than the channel formed with wild-type αHL. The asymmetry of the D108C channel mutant is only slightly larger than that of the wild-type αHL channel, whereas the asymmetry of the I7C channel was practically unaltered.

Based on the results above, we suggest that the net integrated charge is responsible for cation-anion selectivity of the αHL channel, whereas the balance of charges between the openings is crucial for determining the asymmetry of the *G-V* curves. To test this hypothesis, we used reagents that interact specifically with the sulfhydryl group of cysteine and that add either a full positive or negative charge at each cysteine side chain.

Cysteine derivatization and *G-V* dependencies

The conversion of the weak negative charge on cysteine to either a more negative or positive value should produce significant changes in the local electrostatic potential profile. In an attempt to affect such changes, each of the point cysteine mutants was subjected to targeted chemical modification with specific sulfhydryl reagents. These experiments were conducted with preformed heptameric channels and channels formed by chemically modified monomers of αHL. The reagents (when applied on the preinserted channels) rapidly affected the channel conducting properties, and new steady-state values were reached within minutes. Changes in the channel conductance and rectification after reagent application served as a criterion for judging the accessibility of the sulfhydryl group. The effect was evident in bilayers that contained either multiple or single channels. In the case of multiple channels, the reagent-induced change to the membrane current was smooth (data not shown) and reflected the aggregate change in the conductance of individual ion channels. Similar to our findings in an earlier study (24), the

reagents caused abrupt, cascade-like changes in the channel conductance (Fig. 7 *A*), suggesting the rapid, consecutive modification of the cysteines within the individual heptameric pores. The time-resolved cascade of changes in conductance could be observed in the presence of relatively small reagent concentration (24). Here, our goal was to rapidly derivatize the available sites (Fig. 7 *B*). It needs to note that the rate of the cysteine derivatization depends on the type of reagent also. The rate was higher with MTS reagents than with DTNB. When the steps were resolved, the time interval between them varied from channel to channel, reflecting the stochastic nature of the process. As was shown elsewhere (24) the maximum number of the stepwise changes in the αHL channel conductance was seven. In general, the number of steps we observed was <7. When channels reached the new level of conductance in <7 steps, some of the steps were approximately twice (or more) the magnitude of single steps (Fig. 7 *A*). We assume these events correspond to the simultaneous modification of two or more sulhydryl groups. The seven stepwise changes in channel conductance confirm that α-toxin channel is a heptamer and suggests that all cysteines in the channel are derivatized by the reagents. The conclusion was confirmed with experiments in which mutated αHL monomers were first exposed to an excess of one of the sulfhydryl reagents and then allowed to form channels. For all mutants with a cysteine at an odd-numbered position in the stem region, both chemical modification methods gave virtually identical results. We therefore conclude that all seven novel cysteines for each of these mutants are accessible to, and modified by, the reagents. The effects of sulfhydryl reagents could always be reversed by DTT, and the channels then exhibited properties identical to those of the unmodified mutated toxins. This result confirms that the changes are the result of the reversible modification of the sulfhydryl groups and not due to an irreversible conformational change of the channel.

The shape and the rectification of the preinserted, assembled oligomeric channel formed by mutated αHL treated with MTSES and MTSET at low ionic strength (100 mM KCl) are shown in Figs. 8 and 9. The effects of DTNB and MTSEA were analogous to those of MTSES and MTSET, respectively (data not shown). Specifically, the addition of full negative charges (sulfate or carboxyl groups, MTSES or

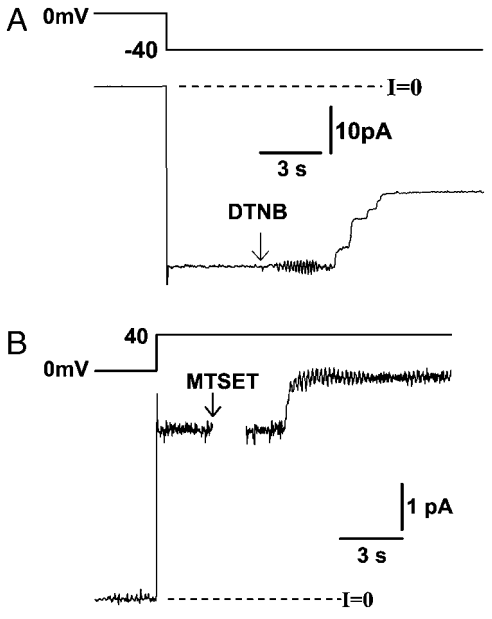

FIGURE 7 Single-channel recordings of G143C-αHL channels before and after the addition of the sulfhydryl reagents DTNB and MTSET. G143C was added to the *cis* solution at a concentration of ~0.2 ng/ml. After a single channel appeared, DTNB (*A*) or MTSET (*B*) was added at a concentration of 1.5 mM and 1 mM to the *cis* and *trans* compartments, respectively. After a few seconds, the channel conductance changed in a stepwise manner (*A*) or smoothly (*B*), indicative of its reaction with reagents. Several clearly resolved steps can be seen in *A*. Solutions in both compartments of the chamber contained KCl (1000 mM (*A*) or 100 mM (*B*)), 0.5 mM DTT, 1 mM EDTA, 30 mM Tris-HCl, pH 7.5. The pulse protocol is shown in the top part of the figure. In each case, the sign of applied potential was chosen to make the greatest possible reagent-induced change in the channel conductance.

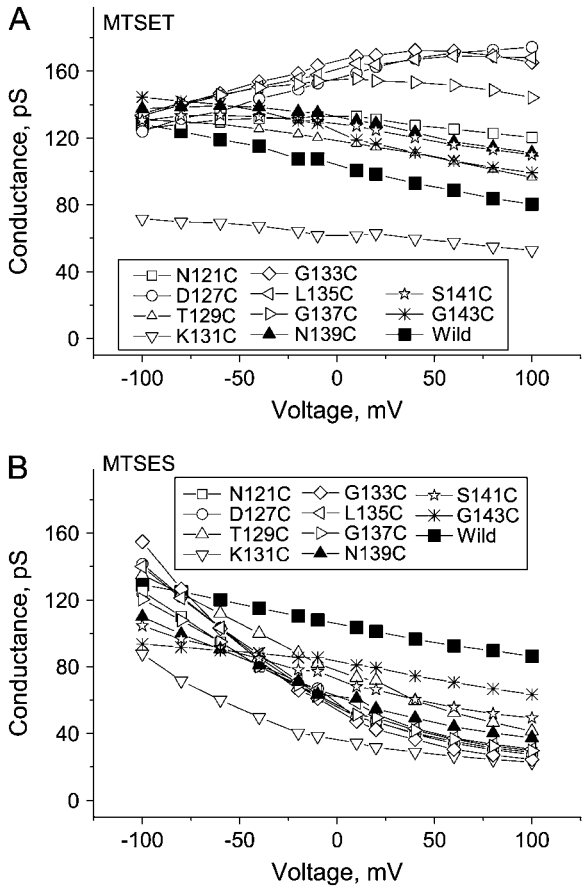

FIGURE 8 Conductance-voltage relationships of channels formed by the odd-numbered single cysteine αHL mutants derivatized by MTSET (*A*) and MTSES (*B*). The SH reagents are added to both bilayer chamber compartments. Each curve represents the mean of three independent experiments. The standard deviation values (not shown) do not exceed 10%.

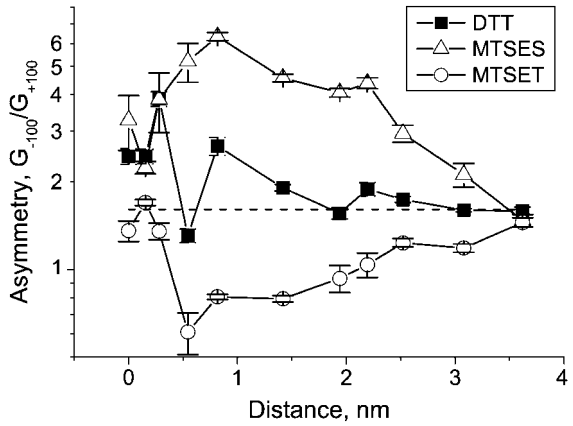

FIGURE 9 Effect of sulfhydryl reagents on the αHL cysteine mutant channel rectification. Each point represents the mean rectification ratio, $G_{-100\ mV}/G_{+100\ mV}$, obtained in 3–5 separate experiments. The dashed line represents the value of G_{-100}/G_{+100} for the wild-type αHL channel. The sequence of mutants from left to right is T129C, G130C, K131C, D127C, G133C, L135C, G137C, N121C, N139C, S141C, and G143C.

DTNB, respectively) in the stem region made the *G-V* curves more asymmetric, and full positive charges (trimethylammonium or amino groups, MTSET or MTSEA, respectively) decreased the rectification. Also, the influence of these novel full charges depends on the position of the charged group. The effect is not particularly strong for charges added at the *trans* entrance. However, the effect first increases as the charges are located into the pore (reaching its maximum value at ~1 nm from the *trans* opening) and then decreases at distances >3 nm.

In contrast, the results obtained with the even numbered mutants were more complex. Except for G130C, sulfhydryl groups at these positions were not always accessible in preformed channels. However, chemical modification of monomeric αHL mutants before channel formation demonstrated that some even-numbered positions (i.e., 124, 126, 128, 132, 134, 136, 138, and 108) are accessible to the reagents because such derivatized mutants form channels with properties considerably different from those of channels formed by original monomeric αHL mutants (data not shown). Apparently, at those particular positions, the charged moieties introduced by the sulfhydryl (SH)-specific reagents cannot be accommodated. The subsequent addition of DTT to these channels did not reverse the effects of derivatization by sulfhydryl agents.

Some of the other even-numbered αHL mutants (i.e., Y118C, F120C, G122C, and V140C) are relatively insensitive to the reagents, even in monomeric form. In contrast, the sulfhydryl group of Cys-130 was accessible in monomeric αHL (aqueous solution) and in preformed channels.

The I7C channel was also sensitive to the reagents. In contrast to the stem region, the introduction of a strong negative charge by DTNB and/or MTSES in the cap domain made the *G-V* curves less asymmetric. The corresponding rectification ratios were 1.55 ± 0.06 and 1.1 ± 0.02, respectively. An attempt to introduce a positive charge at this position of the preformed channel with MTSEA and MTSET was apparently unsuccessful. In that case, we did not observe a significant change in the rectification. The positive charge on Lys-8 may electrostatically repel the positively charged reagent. The effects of the negatively charged sulfhydryl reagents on the I7C mutants were reversed by DTT.

Cysteine derivatization and cation-anion selectivity

The effects of charge introduction on cation-anion selectivity of the αHL channel are summarized in Fig. 10. In this set of

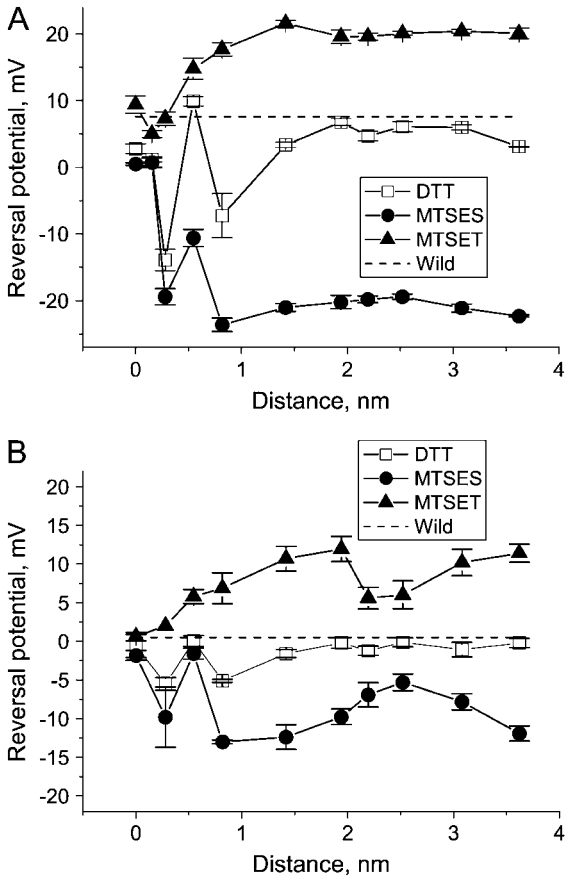

FIGURE 10 Effects of sulfhydryl reagents on the reversal potential of channels formed by single cysteine αHL mutants. (*A*) The membrane is bathed by 100 mM and 300 mM KCl aqueous solution on the *trans* and *cis* sides, respectively. (*B*) 3000 mM/1000 mM (*cis*/*trans*) KCl gradient is used. The maximum and minimum values of P_K/P_{Cl} were 3.0 and 0.35 and were caused by MTSES and MTSET, respectively. The sequence of mutants from left to right is T129C, G130C, K131C, D127C, G133C, L135C, G137C, N121C, N139C, S141C, and G143C. Except for G130C, all other channels formed by even-numbered point cysteine mutants, including D108C, were insensitive to the SH reagents. The dashed line represents the value of the reversal potential for the channel formed by wild-type αHL. Each point represents the mean value (± SD) of V_{rev} obtained in 5–7 independent experiments.

the experiments, the channels were first formed by mutant αHL in lipid bilayer membranes, and then water-soluble sulfhydryl-specific reagents were applied. The cysteines at even-numbered positions were virtually inaccessible to SH reagents. A weak change in the channel selectivity was observed only in the case of Cys-130, which is located close to the *trans* entrance.

As expected, selectivity changes were observed for all odd-numbered sites in the stem region that we tested. The data provide additional support for the β-barrel structure of the pore-forming stem region (23,60). The extent of the selectivity changes caused by the chemical derivatization was virtually identical to that obtained with channels formed by the same odd-numbered mutants derivatized in monomeric form in aqueous solution. The effectiveness of the novel charges was dependent on their location along the channel axis. Relatively weak effects were found for charges located close to the channel opening. The effect of charges increased with distance, and at a distance of 1–1.5 nm from the *trans* opening (i.e., the end opposite the large cap domain of αHL) V_{rev} was maximal at ~+21 mV (MTSET) or at −24 mV (MTSES), with relative permeability ratios, P_K/P_{Cl}, of ~0.001 and ~170, respectively, whereas wild αHL channel is weakly anion-selective with V_{rev} ~ 7.6 mV and P_K/P_{Cl} ~ 0.46. The maximal values of V_{rev} for the derivatized αHL channels are close to the Nernst potentials (~+22 mV and ~−25 mV for Cl^- and K^+, respectively). Thus, the derivatized αHL channels are highly selective for anions or cations, depending on the sign of the novel charge. Charges located further in the pore interior have a greater influence on selectivity.

The position of the novel charge affects V_{rev} and the asymmetry of *G-V* curves differently. After an initial increase, V_{rev} remains large and nearly constant (Fig. 10 *A*). In contrast, the change in the asymmetry vanishes quickly with distance from the *trans* pore entrance (Fig. 9). The results suggest that the net (integrated) charge is responsible for cation-anion selectivity of the αHL channel, whereas the balance of charges between the openings is crucial for determining the *G-V* curves.

The introduction of a strong negative charge (i.e., with DTNB or MTSES reagents) into the cap domain (I7C channel) changes the channel selectivity in a manner consistent with modification of the stem region (the channel became more cation-selective). The change in V_{rev} (from 7.6 ± 0.7 mV to 5.8 ± 0.7 mV) was moderate, but statistically reliable ($P < 0.05$). The large pore radius in the cap region may be responsible for the less striking result. As mentioned above, the positively charged reagents (i.e., MTSET and MTSEA) caused no discernable effects on I7C channel properties.

Stem radius and the charge effectiveness

The long-range action of a charge depends on the ionic strength of the supporting electrolyte and may be described approximately with the Debye equation for planar surfaces. Thus, the placement of charges close to the pore openings will be readily affected by changes in the bulk ionic strength. How far into the pore would changes in the bulk aqueous solution be felt? To address this question, the reversal potential was also measured in the presence of a 3000 mM/1000 mM (*cis*/*trans*) KCl gradient (Fig. 10 *B*). In contrast to the results obtained at lower KCl concentration (Fig. 10 *A*), the V_{rev}-distance dependencies have a minimum at ~2.5 nm from the *trans* opening. This behavior was considerably different from that observed at low salt concentrations for the point cysteine mutants (Fig. 6). We draw two conclusions: the increase in KCl concentration in bathing solution decreases the long-range action of the charges even though they are far from the opening, and that additional factor(s) contributed to the value of the reversal potential, V_{rev}. As shown above, a ring of charge introduced into the wider cap vestibule caused only slight changes to the αHL channel conducting properties. Are the charges added to the stem region located at a different distance from the channel axis? The stem of αHL channel is a right hand β-barrel. The radius, measured from α-carbon positions, is assumed to be ~1.3 nm. However, the detailed analysis of the channel radii at each of the odd-numbered side-chain α-carbon atoms, performed with the Swiss-Pdb Viewer version 3.7 (49) and CS Chem3D Pro, demonstrates that they are not constant. The variation of the radius with distance from the *trans* pore entrance is nearly a mirror image of the distance dependence of V_{rev} (Fig. 11 *A*). Thus, there is an inverse correlation between these two parameters (Fig. 11 *B*), which suggests that the geometry determines the effectiveness of the charges even in such confined spaces as water-filled pores of nanometer dimensions.

SUMMARY AND CONCLUSIONS

We used cysteine-scanning mutagenesis to better understand the basis of ion selectivity and ionic current rectification in a channel with a known three-dimensional structure. The aim of this study was to determine experimentally the significance of both the charge type and its position within the ion conduction pathway on the selectivity, conductance, and *G-V* lineshape of the αHL channel. The choice of αHL channel was also motivated by its potential importance for biotechnology applications.

Several attempts were earlier made to describe theoretically these αHL channel properties, where qualitative (28,35) or nearly quantitative (19) descriptions were achieved assuming that the fixed charges inside the pore and near the pore's entrances affect the channel properties. We have determined the *G-V* relationship and cation-anion selectivity of channels using 24 cysteine-substituted αHL mutants with or without derivatization of Cys with sulfhydryl-specific water-soluble reagents. The conditions we used (low ionic strength and net neutral planar lipid membranes) were optimal for revealing even the influence of weak charges. In

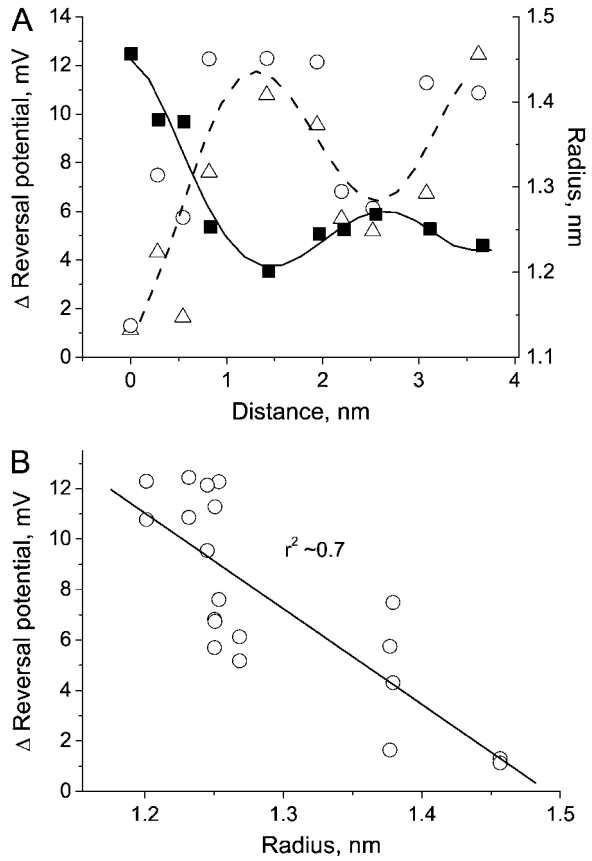

FIGURE 11 Interrelation between the variation of the reversal potential of ion channels formed by cysteine-substituted derivatized αHL mutants and the radius of the wild-type channel. (*A*) The variation of the reversal potential (○, △) of ion channels built by cysteine-substituted derivatized αHL mutants and the radius (■) of the channel with the distance from the *trans* opening . △, MTSES treatment; ○, MTSET treatment. The data are the absolute value of the difference in V_{rev} of ion channels before and after derivatization in the presence of a 3000 mM/1000 mM (*cis*/*trans*) KCl gradient. Each point represents the mean values obtained in 5–7 separate experiments. The sequence of mutants from left to right is as follows: T129C, K131C, D127C, G133C, L135C, G137C, N121C, N139C, S141C, G143C. The radii were determined from the α-carbon of each odd amino acid residue in the stem region using the αHL channel crystallographic structure (7AHL.pdb), the Swiss-Pdb Viewer version 3.7 (49), and CS Chem3D Pro (CambridgeSoft). (*B*) The correlation between the variation of the reversal potential and the radii of channels formed by point cysteine mutants.

this study, we demonstrate how the magnitude of the effect of charges depends on the position of the charges along the longitudinal channel axis.

The selectivity and the asymmetry of the conductance-voltage relationship of αHL channel depends on the bulk aqueous solution ionic strength, which suggests that the charges facing the aqueous phase inside the nanoscopic pore play a key role in determining these channel properties. Among the 24 point cysteine mutants reported here, only six mutations that are close to the *trans* opening (i.e., positions 126, 128, 129, 130, 131, and 133 in the stem region) have a significant influence on the channel conductance. Except at position 130 and positions 128 and 131, none of the other three mutations were reported previously to have a major effect on αHL channel properties without chemical modification.

Sulfhydryl-specific water-soluble reagents changed the properties of preinserted, assembled oligomeric channels formed by odd-numbered mutants with Cys in the stem region. Among the channels formed by even-numbered mutants, the G130C channel was unique in having properties that were altered by the reagents. The changes in properties of preinserted channels are most likely the result of the addition of novel fixed charges to the pore wall (the effects of sulfhydryl reagents on these mutants could always be reversed by DTT).

The treatment of monomeric αHL mutants with specific sulfhydryl reagents in solution before channel formation demonstrated that some even-numbered positions (124, 126, 128, 132, 134, 136, 138, and 108) form channels with properties considerably different from those of channels formed by original monomeric αHL mutants. In the case of these derivatized even-numbered mutants, the effects of sulfhydryl reagents could not be reversed by treatment of the channels with DTT. Some of the other even-numbered αHL mutants (Y118C, F120C, G122C, and V140C) appear to be insensitive to the reagents.

The effectiveness of the novel charges depends on both their type and location along the channel axis. The introduction of a strong negative charge in the *trans* part of the pore (stem region) made the channel more selective to cations and increased the asymmetry of the *G-V* curve. In contrast, the introduction of a positive charge had the opposite effect. Relatively weak effects were observed for mutants with charges located close to the channel openings. The effect of charges initially increased with distance from the *trans* opening and had a maximum influence on the asymmetry of *G-V* curves or saturated close to the Nernst potentials (V_{rev}) at a distance of 0.8–1.5 nm from the *trans* opening. Thus, it is possible to create an ion-selective filter for relatively large water-filled pores of nanometer dimensions by the introduction of a ring of charge. The charges have to be located in regions with smaller radii inside the pore to have a stronger influence on the αHL channel selectivity and to be located close to pore openings to affect the channel *G-V* dependence. These charged rings not only affect *G-V* dependence and the channel's selectivity to small mobile charges, they also have a strong influence on polynucleotide transport through the αHL channel (S. E. Henrickson, O. V. Krasilnikov, A. Valeva, and J. J. Kasianowicz, unpublished observations).

In contrast to the results obtained with charges added to the stem region, the introduction of a negative charge in the cap domain made the *G-V* curves less asymmetric and the channel more cation-selective. The results suggest that the net (integrated) charge is responsible for cation-anion selectivity

of the αHL channel, whereas the balance of charges between the openings is crucial for determining the *G-V* curves.

An increase in the KCl concentration in the bulk determines the mobile charge concentration within the channel. The mobile charges screen the fixed charges added to the pore wall, even when they are relatively far from the pore entrances.

The stem region of αHL channel is a right-hand β-barrel. However, the radius, measured from α-carbon positions of each odd amino acid residue in the stem, is not constant. The value of the radius deduced from the crystal structure correlates inversely with the effectiveness of the novel charges on ion selectivity. Thus, the local properties of the channel influence the effectiveness of the charges in an ion channel with nanometer-scale dimensions. We expect that the results obtained here will be applicable to other biological or synthetic water-filled nanopores.

We are grateful to Dr. Elbert Lee (National Institute for Physiological Sciences, Okazaki, Japan) for helpful suggestions on the manuscript. Inclusion of suppliers and manufacturers of materials and equipment is for completeness and does not constitute endorsement by the National Institute of Standards and Technology. This work is dedicated to the memory of Professor Gianfranco Menestrina, one of the pioneers in the study of pore-forming toxins.

This study was partially supported by Conselho National de Desenvolvimento Cientifico e Tecnologico (Brazil). This work was sponsored in part by the National Institute of Standards and Technology Advanced Technology Program, and the National Institute of Standards and Technology ''Single Molecule Manipulation and Measurement'' program, and the National Science Foundation (Nanoscale Interdisciplinary Research Team grant CTS-0304062).

REFERENCES

1. Hille, B. 1992. Ionic channels of excitable membranes. Sinauer Associates, Sunderland, MA.
2. Krasilnikov, O. V., P. G. Merzliak, R. Z. Sabirov, and B. A. Tashmukhamedov. 1990. Memory is a property of an ion channels pool—ion channels formed by *Staphylococcus aureus* α-toxin. *Gen. Physiol. Biophys.* 9:569–575.
3. Bezrukov, S. M., and J. J. Kasianowicz. 1993. Current noise reveals protonation kinetics and number of ionizable sites in an open protein ion channel. *Phys. Rev. Lett.* 70:2352–2355.
4. Kasianowicz, J. J., and S. M. Bezrukov. 1995. Protonation dynamics of the α-toxin ion-channel from spectral-analysis of pH-dependent current fluctuations. *Biophys. J.* 69:94–105.
5. Kasianowicz, J. J., E. Brandin, D. Branton, and D. W. Deamer. 1996. Characterization of individual polymucleotide molecules using a membrane channel. *Proc. Natl. Acad. Sci USA.* 93:13770–13773.
6. Cornell, B. A., V. L. B. Braach-Maksvytis, L. G. King, P. D. J. Osman, B. Raguse, L. Wieczorek, and R. J. Pace. 1997. A biosensor that uses ion-channel switches. *Nature.* 387:580–583.
7. Braha, O., B. Walker, S. Cheley, J. J. Kasianowicz, L. Z. Song, J. E. Gouaux, and H. Bayley. 1997. Designed protein pores as components for biosensors. *Chem. Biol.* 4:497–505.
8. Kasianowicz, J. J., D. L. Burden, L. C. Han, S. Cheley, and H. Bayley. 1999. Genetically engineered metal ion binding sites on the outside of a channel's transmembrane β-barrel. *Biophys. J.* 76:837–845.
9. Kasianowicz, J. J., S. E. Henrickson, H. H. Weetall, and B. Robertson. 2001. Simultaneous multianalyte detection with a nanometer-scale pore. *Anal. Chem.* 73:2268–2272.
10. Kasianowicz, J. J., S. E. Henrickson, M. Misakian, H. H. Weetall, B. Robertson, and V. Stanford. 2002. Physics of DNA threading through a nanometer pore and applications to simultaneous multianalyte sensing. *In* Structure and Dynamics of Confined Polymers. J. J. Kasianowicz, M. Kellermayer, and D. W. Deamer, editors. Kluwer Academic Publishers, Dordrecht, The Netherlands. 141–163.
11. Bayley, H., and L. Jayasinghe. 2004. Functional engineered channels and pores (Review). *Mol. Membr. Biol.* 21:209–220.
12. Li, J., D. Stein, C. McMullan, D. Branton, M. J. Aziz, and J. A. Golovchenko. 2001. Ion-beam sculpting at nanometre length scales. *Nature.* 412:166–169.
13. Harrell, C. C., S. B. Lee, and C. R. Martin. 2003. Synthetic Single-nanopore and nanotube membranes. *Anal. Chem.* 75:6861–6867.
14. Storm, A. J., J. H. Chen, X. S. Ling, H. W. Zandbergen, and C. Dekker. 2003. Fabrication of solid-state nanopores with single-nanometre precision. *Nat. Mater.* 2:537–540.
15. Yang, J., F. Lu, L. W. Kostiuk, and D. Y. Kwok. 2003. Electrokinetic microchannel battery by means of electrokinetic and microfluidic phenomena. *J. Micromech. Microeng.* 13:963–970.
16. Adcock, C., G. R. Smith, and M. S. P. Sansom. 1998. Electrostatics and the ion selectivity of ligand-gated channels. *Biophys. J.* 75:1211–1222.
17. Wilson, G. G., J. M. Pascual, N. Brooijmans, D. Murray, and A. Karlin. 2000. The intrinsic electrostatic potential and the intermediate ring of charge in the acetylcholine receptor channel. *J. Gen. Physiol.* 115:93–106.
18. Keramidas, A., A. J. Moorhouse, P. R. Peter, and P. H. Barry. 2004. Ligand-gated ion channels: mechanisms underlying ion selectivity. *Prog. Biophys. Mol. Biol.* 86:161–204.
19. Noskov, S. Y., W. Im, and B. Roux. 2004. Ion permeation through the α-hemolysin channel: Theoretical studies based on Brownian dynamics and Poisson-Nernst-Plank electrodiffusion theory. *Biophys. J.* 87:2299–2309.
20. Jordan, P. C. 2005. Fifty years of progress in ion channel research. *IEEE Trans. Nanobioscience.* 4:3–9.
21. Bhakdi, S., and J. Tranum-Jensen. 1991. Alpha-toxin of *Staphylococcus Aureus. Microbiol. Rev.* 55:733–751.
22. Gouaux, J. E., O. Braha, M. R. Hobaugh, L. Z. Song, S. Cheley, C. Shustak, and H. Bayley. 1994. Subunit stoichiometry of Staphylococcal α-hemolysin in crystals and on membranes: a heptameric transmembrane pore. *Proc. Natl. Acad. Sci. USA.* 91:12828–12831.
23. Song, L. Z., M. R. Hobaugh, C. Shustak, S. Cheley, H. Bayley, and J. E. Gouaux. 1996. Structure of staphylococcal α-hemolysin, a heptameric transmembrane pore. *Science.* 274:1859–1866.
24. Krasilnikov, O. V., P. G. Merzlyak, L. N. Yuldasheva, C. G. Rodrigues, S. Bhakdi, and A. Valeva. 2000. Electrophysiological evidence for heptameric stoichiometry of ion channels formed by *Staphylococcus aureus* α-toxin in planar lipid bilayers. *Mol. Microbiol.* 37:1372–1378.
25. Krasilnikov, O. V., R. Z. Sabirov, V. I. Ternovsky, P. G. Merzliak, and B. A. Tashmukhamedov. 1988. The structure of *Staphylococcus aureus* α-toxin-induced ionic channel. *Gen. Physiol. Biophys.* 7:467–473.
26. Krasilnikov, O. V. 2002. Sizing channels with neutral polymers. *In* Structure and Dynamics of Confined Polymers. J. J. Kasianowicz, M. S. Z. Kellermayer, and D. W. Deamer, editors. Kluwer Academic Publishers, Dordrecht, The Netherlands. 97–115.
27. Füssle, R., S. Bhakdi, A. Sziegoleit, J. Tranum-Jensen, T. Kranz, and H. J. Wellensiek. 1981. On the mechanism of membrane damage by *Staphylococcus aureus* α-toxin. *J. Cell Biol.* 91:83–94.
28. Krasilnikov, O. V., and R. Z. Sabirov. 1989. Ion transport through channels formed in lipid bilayers by *Staphylococcus aureus* α-toxin. *Gen. Physiol. Biophys.* 8:213–222.

29. Howorka, S., L. Movileanu, X. F. Lu, M. Magnon, S. Cheley, O. Braha, and H. Bayley. 2000. A protein pore with a single polymer chain tethered within the lumen. *J. Am. Chem. Soc.* 122: 2411–2416.

30. Merzlyak, P. G., L. N. Yuldasheva, C. G. Rodrigues, C. M. M. Carneiro, O. V. Krasilnikov, and S. M. Bezrukov. 1999. Polymeric nonelectrolytes to probe pore geometry: Application to the α-toxin transmembrane channel. *Biophys. J.* 77:3023–3033.

31. Movileanu, L., S. Cheley, S. Howorka, O. Braha, and H. Bayley. 2001. Location of a constriction in the lumen of a transmembrane pore by targeted covalent attachment of polymer molecules. *J. Gen. Physiol.* 117:239–251.

32. Krasilnikov, O. V., V. I. Ternovsky, and B. A. Tashmukhamedov. 1981. Properties of α-staphylotoxin-induced conductivity channels in bilayer phospholipid-membranes. *Biofizika.* 26:271–276.

33. Menestrina, G. 1986. Ionic channels formed by *Staphylococcus aureus* α-toxin: voltage-dependent inhibition by divalent and trivalent cations. *J. Membr. Biol.* 90:177–190.

34. Krasilnikov, O. V., V. I. Ternovsky, R. Z. Sabirov, R. K. Zaripova, and B. A. Tashmukhamedov. 1986. Cation-anion selectivity of staphylotoxin channels in lipid bilayer. *Biofizika.* 31:606–610.

35. Misakian, M., and J. J. Kasianowicz. 2003. Electrostatic influence on ion transport through the α HL channel. *J. Membr. Biol.* 195:137–146.

36. Noskov, S. Y., S. Berneche, and B. Roux. 2004. Control of ion selectivity in potassium channels by electrostatic and dynamic properties of carbonyl ligands. *Nature.* 431:830–834.

37. Bezrukov, S. M., I. Vodyanoy, R. A. Brutyan, and J. J. Kasianowicz. 1996. Dynamics and free energy of polymers partitioning into a nanoscale pore. *Macromolecules.* 29:8517–8522.

38. Bezrukov, S. M., and J. J. Kasianowicz. 2002. Dynamic partitioning of neutral polymers into a single ion channel. *In* Structure and Dynamics of Confined Polymers. J. J. Kasianowicz, M. S. Z. Kellermayer, and D. W. Deamer, editors. Kluwer Academic Publishers, Dordrecht, The Netherlands. 117–130.

39. Krasilnikov, O. V., and S. M. Bezrukov. 2004. Polymer partitioning from nonideal solutions into protein voids. *Macromolecules.* 37:2650–2657.

40. Kasianowicz, J. J. 2004. Nanopores: flossing with DNA. *Nat. Mater.* 3:355–356.

41. Bezrukov, S. M., O. V. Krasilnikov, L. N. Yuldasheva, A. M. Berezhkovskii, and C. G. Rodrigues. 2004. Field-dependent effect of crown ether (18-crown-6) on ionic conductance of α-hemolysin channels. *Biophys. J.* 87:3162–3171.

42. Bezrukov, S. M., and J. J. Kasianowicz. 1997. The charge state of an ion channel controls neutral polymer entry into its pore. *Eur. Biophys. J.* 26:471–476.

43. Akabas, M. H., D. A. Stauffer, M. Xu, and A. Karlin. 1992. Acetylcholine-receptor channel structure probed in cysteine-substitution mutants. *Science.* 258:307–310.

44. Montal, M., and P. Mueller. 1972. Formation of bimolecular membranes from lipid monolayers and a study of their electrical properties. *Proc. Natl. Acad. Sci. USA.* 69:3561–3566.

45. Krasilnikov, O. V., P. G. Merzliak, L. N. Yuldasheva, R. A. Nogueira, and C. G. Rodrigues. 1995. Non stochastic distribution of single channels in planar lipid bilayers. *Biochim. Biophys. Acta.* 1233: 105–110.

46. Barry, P. H., and J. W. Lynch. 1991. Liquid junction potentials and small-cell effects in patch-clamp analysis. *J. Membr. Biol.* 121:101–117.

47. Ng, B., and P. H. Barry. 1995. The measurement of ionic conductivities and mobilities of certain less common organic ions needed for junction potential corrections in electrophysiology. *J. Neurosci. Methods.* 56: 37–41.

48. Valeva, A., J. Pongs, S. Bhakdi, and M. Palmer. 1997. Staphylococcal α-toxin: the role of the N-terminus in formation of the heptameric pore—a fluorescence study. *Biochim. Biophys. Acta.* 1325:281–286.

49. Guex, N., and M. C. Peitsch. 1997. SWISS-MODEL and the Swiss-PdbViewer: an environment for comparative protein modeling. *Electrophoresis.* 18:2714–2723.

50. Neumcke, B. 1970. Ion flux across lipid bilayer membranes with charged surfaces. *Biophysik.* 6:231–240.

51. Markin, V. S., and Y. A. Chismadjev. 1974. Induced Ion Transport. Nauka, Moscow.

52. Bell, J. E., and C. Miller. 1984. Effects of phospholipid surface-charge on ion conduction in the K^+ channel of sarcoplasmic-reticulum. *Biophys. J.* 45:279–287.

53. Krasilnikov, O. V., M. F. P. Capistrano, L. N. Yuldasheva, and R. A. Nogueira. 1997. Influence of Cys-130 S-aureus α-toxin on planar lipid bilayer and erythrocyte membranes. *J. Membr. Biol.* 156:157–172.

54. Krasilnikov, O. V., P. G. Merzlyak, R. Z. Sabirov, V. I. Ternovsky, and R. K. Zaripova. 1988. Influence of pH on the potential-dependence of Staphylococcal toxin channels functioning in phosphatidylcholine bilayer. *Ukr. Biokhim. Zh.* 60:60–66.

55. Krasilnikov, O. V., L. N. Yuldasheva, P. G. Merzlyak, M. F. P. Capistrano, and R. A. Nogueira. 1997. The hinge portion of the *S. aureus* α-toxin crosses the lipid bilayer and is part of the *trans*-mouth of the channel. *Biochim. Biophys. Acta.* 1329:51–60.

56. Korchev, Y. E., C. L. Bashford, G. M. Alder, J. J. Kasianowicz, and C. A. Pasternak. 1995. Low-conductance states of a single-ion channel are not closed. *J. Membr. Biol.* 147:233–239.

57. Krasilnikov, O. V., P. G. Merzlyak, L. N. Yuldasheva, C. G. Rodrigues, and R. A. Nogueira. 1999. Heparin influence on α-staphylotoxin formed channel. *Biochim. Biophys. Acta.* 1417:167–182.

58. Krasilnikov, O. V., P. G. Merzlyak, L. N. Yuldasheva, and R. A. Nogueira. 1998. Channel-sizing experiments in multichannel bilayers. *Gen. Physiol. Biophys.* 17:349–363.

59. Krekel, F., A. K. Samland, P. Macheroux, N. Amrhein, and J. N. S. Evans. 2000. Determination of the pK(a) value of C115 in MurA (UDP-*N*-acetylglucosamine enolpyruvyltransferase) from *Enterobacter cloacae*. *Biochemistry.* 39:12671–12677.

60. Valeva, A., A. Weisser, B. Walker, M. Kehoe, H. Bayley, S. Bhakdi, and M. Palmer. 1996. Molecular architecture of a toxin pore: a 15-residue sequence lines the transmembrane channel of staphylococcal α-toxin. *EMBO J.* 15:1857–1864.